

International Journal of Engineering Sciences & Research Technology

(A Peer Reviewed Online Journal)

Impact Factor: 5.164



Chief Editor

Dr. J.B. Helonde

Executive Editor

Mr. Somil Mayur Shah

ABSTRACT

In this thesis, a method for forward and inverse kinematics analysis of a 5-DOF and a 7-DOF Redundant manipulator is proposed. Obtaining the trajectory and computing the required joint angles for a higher DOF robot manipulator is one of the important concerns in robot kinematics and control. When a robotic system possesses more degree of freedom (DOF) than those required to execute a given task is called Redundant Manipulator. The difficulties in solving the inverse kinematics (IK) equations of these redundant robot manipulator arises due to the presence of uncertain, time varying and non-linear nature of equations having transcendental functions. In this thesis, the ability of ANFIS (Adaptive Neuro-Fuzzy Inference System) is used to the generated data for solving inverse kinematics problem. The proposed hybrid neuro-fuzzy system combines the learning capabilities of neural networks with fuzzy inference system for nonlinear function approximation. A single-output Sugeno-type FIS (Fuzzy Inference System) using grid partitioning has been modeled in this work. The Denavit-Hartenberg (D-H) representation is used to model robot links and solve the transformation matrices of each joint. The forward kinematics and inverse kinematics for a 5-DOF and 7-DOF manipulator are analyzed systemically.

ANFIS have been successfully used for prediction of IKs of 5-DOF and 7-DOF Redundant manipulator in this work. After comparing the output, it is concluded that the predicting ability of ANFIS is excellent as this approach provides a general frame work for combination of NN and fuzzy logic. The Efficiency of ANFIS can be concluded by observing the surface plot, residual plot and normal probability plot. This current study in using different nonlinear models for the prediction of the IKs of a 5-DOF and 7-DOF Redundant manipulator will give a valuable source of information for other modellers.

KEYWORDS: 5-DOF and 7-DOF Redundant Robot Manipulator; Inverse kinematics; ANFIS; Denavit-Hartenberg (D-H) notation

1. INTRODUCTION**1.1 Introduction to Robotics**

Word robot was coined by a Czech novelist Karel Capek in 1920. The term robot derives from the Czech word *robota*, meaning forced work or compulsory service. A robot is reprogrammable, multifunctional manipulator designed to move material, parts, tools, or specialized devices through various programmed motions for the performance of a variety of tasks. A simpler version it can be define as, an automatic device that performs functions normally ascribed to humans or a machine in the form of a human.

1.2 History of Robotics

The first industrial robot named UNIMATE; it is the first programmable robot designed by George Devol in 1954, who coined the term Universal Automation. The first UNIMATE was installed at a General Motors plant to work with heated die-casting machines. In 1978, the Puma (Programmable Universal Machine for Assembly) robot is developed by Victor Scheinman at pioneering robot company Unimation with a General Motors design support. These robots are widely used in various organisations such as Nokia corporation, NASA, Robotics and Welding organization.



Figure 1.1 The first industrial robot: UNIMATE



Figure 1.2 Puma Robotic Arm

Then the robot industries enters a phase of rapid growth to till date, as various type of robot are being developed with various new technology, which are being used in various industries for various work. Few of these milestones in the history of robotics are given.

- 1947— The first servoelectric powered teleoperator is developed.
- 1948— A teleoperator is developed incorporating force feedback.
- 1949— Research on numerically controlled milling machine is initiated.
- 1954— George Devol designs the first programmable robot.
- 2007— TOMY (Japanese toy co. Ltd.) launched the entertainment robot, i-robot, which is a humanoid bipedal robot that can walk like a human beings and performs kicks and punches and also some entertaining tricks and special actions under "Special Action Mode".
- 2010— To present, Robonaut 2, the latest generation of the astronaut helpers, launched to the space station aboard Space Shuttle Discovery on the STS-133 mission. It is the first humanoid robot in space, and although its primary job for now is teaching engineers how dexterous robots behave in space, the hope is that through upgrades and advancements, it could one day venture outside the station to help spacewalkers make repairs or additions to the station or perform scientific work.

1.3 Laws of Robotics

- Zeroth Law: A robot may not injure humanity, or, through inaction, allow humanity to come to harm.
- First Law: A robot may not injure a human being, or, through inaction, allow a human being to come to harm, unless this would violate a higher order law.
- Second Law: A robot must obey orders given it by human beings, except where such orders would conflict with a higher order law.
- Third Law: A robot must protect its own existence as long as such protection does not conflict with a higher order law.

1.4 Components and Structure of Robots

The basic components of an industrial robot are:

- ❖ The manipulator
- ❖ The End-Effector (Which is a part of the manipulator)
- ❖ The Power supply
- ❖ The controller

Robot Manipulators are composed of links connected by joints into a kinematic chain. Joints are typically rotary (revolute) or linear (prismatic). A revolute joint rotates about a motion axis and a prismatic joint slide along a motion axis. It can also be define as a prismatic joint is a joint, where the pair of links makes a translational displacement along a fixed axis. In other words, one link slides on the other along a straight line. Therefore, it is also called a sliding joint. A revolute joint is a joint, where a pair of links rotates about a fixed axis. This type of joint is often referred to as a hinge, articulated, or rotational joint. The controller initiates, terminates, and coordinates the motion of sequences of a robot. Also it accepts the necessary inputs to the robot and provides the outputs to interface with the outside world. In other words the controller processes the sensory information and computes the control commands for the actuator to carry out specified tasks

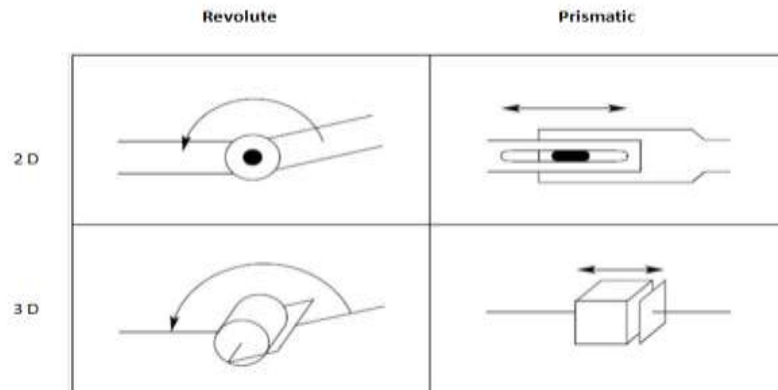


Figure 1.4. Symbolic representation of robot joints.

1.5 Redundant Manipulator

A manipulator is required have a minimum of six degree of freedom if it needs to acquire any random position and orientation in its operational space or work space. Assuming one joint is required for each degree of freedom, such a manipulator needs to be composed of minimum of six joints. Usually in standard practice three degree of freedom is implemented in the robotic arm so it can acquire the desired position in its work space. The arm is then fitted with a wrist composed of three joints to acquire the desired orientation. Such a manipulator is called non-redundant. Though non-redundant manipulators are kinematically simple to design and solve, but the non-redundancy leads to two fundamental problems: singularity and inability to avoid obstacles. The singularities of the robot manipulator are present both in the arm and the wrist and can occur anywhere inside the workspace of the manipulator. While passing through these singularities, the manipulator can effectively lose certain degree of freedom, resulting in uncontrollability along those directions. A redundant manipulator offer several potential advantages over a non-redundant manipulator. The extra DOF that require for the free positioning of manipulator can be used to move around or between obstacles and thereby to manipulate in situations that otherwise would be inaccessible. Due to the redundancy the manipulators become flexible, compliant, extremely dextrous and capable of dynamic adaptive, in unstructured environment.

1.6 Degree of Freedom (DOF)

The number of joints determines the degrees-of-freedom (DOF) of the manipulator. Typically, a manipulator should possess at least six independent DOF: three for positioning and three for orientation. With fewer than six DOF the arm cannot reach every point in its work environment with arbitrary orientation. Certain applications such as reaching around or behind obstacles require more than six DOF. The difficulty of controlling a manipulator. increases rapidly with the number of links. A manipulator having more than six links is referred to as a kinematically redundant manipulator.

1.7 Motivations

The motivation for this thesis is to obtain the inverse kinematic solutions of redundant manipulator such as 5-DOF Redundant manipulator and 7-DOF Redundant manipulator. As the inverse kinematic equation of these types of manipulators contain non-linear equations, time varying equations and transcendental functions. Due to the complexity in solving this type of equation by geometric, iterative or algebraic method is very difficult and time consuming. It is very important to solve the inverse kinematics solution for this type of redundant manipulator to know the exact operational space and to avoid the obstacles. Although ANN are very efficient in adopting and learning but they have the negative attribute of 'black box'. To overcome this drawback, various author adopted neuro fuzzy method like ANFIS (Adaptive Neuro-fuzzy Inference system). This can be justify as ANFIS combines the advantage of ANN and fuzzy logic technique without having any of their disadvantage . The neuro fuzzy system are must widely studied hybrid system now a days, as due to the advantages of two very important modelling technique i.e. NN and Fuzzy logic. So the goal of this thesis is to predict the inverse kinematics solution for the redundant manipulator using ANFIS. As a result suitable posture and the trajectories for the manipulator can be planned for execution of different work in various fields.

1.8 Objectives of the Thesis

The objective of this thesis is to solve the inverse kinematics equations of the redundant manipulator. The inverse kinematics equations of this type of manipulator are highly unpredictable as this equation are highly non-linear and contains transcendental function. The complexity in solving this equation increases due to

increase in higher DOF. So various authors had used neuro-fuzzy method (ANFIS) to solve the non-linear and complex equations. arise in different field. ANFIS was adopted by different researcher in their work, for mathematical modelling of the data, as it have high range of potential for solving the complex and nonlinear equations arise in different field like in marketing, manufacturing industries, civil engineering etc.

The main objectives of this thesis can be summarized as:

- The difficulties in solving the Inverse kinematics (IK) of the redundant manipulator increases, as the IK equations possess an infinite number of solutions due to the presence of uncertain, time varying and non-linear nature of these equations having transcendental functions. So in this thesis ANFIS is adopted for estimating the IK solution of a 7-DOF Redundant manipulator.
- The Denavit-Hartenberg (D-H) representation is used to model robot links and solve the transformation matrices of each joint.
- The solution of the IK of redundant manipulator predicted by the ANFIS model is compared with the analytical value. It is found that the predicting ability of ANFIS is excellent. As it is a combination of neural network (NN) and neuro-fuzzy (NF) technique.
- The data predicted with ANFIS for 5-DOF and 7-DOF Redundant manipulator, in this work clearly depicts that the proposed method results in an acceptable error. Hence ANFIS can be utilized to provide fast and acceptable solutions of the inverse kinematics, thereby making ANFIS as an alternate approach to map the inverse kinematic solutions.

1.9 Research methods

The theoretical discussion and results, or the method adopted in this thesis regarding the prediction of inverse kinematics solution of the redundant manipulator have been kept general without reference to any particular manipulator. The purpose is to keep the findings useful for other developments and continue the research and discussion process on a wider scale. In the latter part of the thesis, the ANFIS methodology used for the prediction of IK solution of the redundant manipulator is carried out and the predicted values are verified with the analytical values. The data are trained in ANFIS many times such as to get an appropriate mathematical model. After the training of the data, the predicted values are compared with the analytical value. The residual of the analytical and predicted values are found out and the mean square error, normal probability plot and the regression plots are also carried out. It is concluded that the mean square error and the residual are accepted, thereby making ANFIS as an alternative technique for solving the non-linear equation of redundant manipulator.

2. LITERATURE REVIEW

Obtaining the inverse kinematics solution has been one of the main concerns in robot kinematics research. The complexity of the solutions increases with higher DOF due to robot geometry, non-linear equations (i.e. trigonometric equations occurring when transforming between Cartesian and joint spaces) and singularity problems. Obtaining the inverse kinematics solution requires the solution of nonlinear equations having transcendental functions. In spite of the difficulties and time consuming in solving the inverse kinematics of a complex robot, researchers used traditional methods like algebraic, geometric, and iterative procedures. But these methods have their own drawbacks as algebraic methods do not guarantee closed form solutions. In case of geometric methods, closed form solutions for the first three joints of the manipulator must exist geometrically. The iterative methods converge to only a single solution depending on the starting point and will not work near singularities. A kinematically redundant manipulator is a robotic arm possessing extra degrees of freedom (DOF) than those required to establish an arbitrary position and orientation of the end-effector. A redundant manipulator offers several potential advantages over a non-redundant

They also analysed the limitation of the parameter caused by a joint limit based on a geometric construction. The analysis has its own drawback as priority is being given to one of the wrist joint limits. Based on the closed-form inverse solution and using angle parameters by Dahm and Joubin in his work, Moradi and Lee minimised elbow movement by developing a redundancy resolution method.

Due to the presence of non-linearity, complexity, and transcendental function as well as singularity issues in solving the IK, various researchers used different methods like iteration, geometrical, closed-form inverse solution, redundancy resolution as discussed in above theory. But some researchers also adopted methods like algorithms, neural network, neuro fuzzy in recent years for solving the non-linear equation arising in different areas such as in civil engineering for constitutive modelling, for structural analysis and design, for structural dynamics and control, for non-destructive testing methods of material and many disciplines including business, engineering, medicine, and science. Due to the adapting and learning nature, ANN is an efficient method to solve non-linear

problems. So it has a wide range of application in manufacturing industry, precisely for Electro discharge machining (EDM) process. Various authors had adopted ANN with different training algorithms namely Levenberg-Marquardt algorithm, scaled conjugate gradient algorithm, Orient descent algorithm, Gaussi Netwon algorithm and with different activation fuction like logistic sigmoid, tangent sigmoid, pure lin to model the EDM process. Mandel et.al. used ANN with back propagation as learning algorithm to model EDM process. They concluded that by considering different input parameters such as roughness, material removal rate (MRR), and Tool wear rate (TWR) are found to be efficient for predicting the response parameters. Panda and Bhoi, predicted MRR of D2 grads steel by developing a artificial feed forward NN model based on Levenberg-Marquardt back propagation technique and logistic sigmoid activation function. The model performs faster and provides more accurate result for predicting MRR. Goa et.al. considered different algorithm like L-M algorithm, resilient algorithm, Gausi-Newton algorithm to established different model for machining process. Most of the researchers have studied only a limited numbers of nonlinear model using ANFIS and ANN, as discussed above in the above theory. Despite the widespread application of these nonlinear mathematical models in various field such as in civil engineering, manufacturing industry, marketing field, business field, some authors have carried out a comparison study using different nonlinear models of NN and NF, which gives a valuable.

In the present study, ANFIS is implemented to analyze the kinematics equation of PArm 5-DOF robot manipulator having 6-DOF end-effector and 7-DOF redundant manipulator. Jang reported that the ANFIS can be employed to model nonlinear functions, identify nonlinear components on-line in a control system, and predict a chaotic time series. It is a hybrid neuro-fuzzy technique that brings learning capabilities of neural networks to fuzzy inference systems. The learning algorithm tunes the membership functions of a Mamdani or Sugeno-type Fuzzy Inference System using the training input-output data. According to Jang , ANFIS is divided into two steps. For the first step of consequent parameters training, the least square (LS) method is used and the output of ANFIS is a linear combination of the consequent parameters. After the consequent parameters have been adjusted, the premise parameters are updated by gradient descent principle in the second step. It is concluded that ANFIS use the hybrid learning algorithm that combines least square method with gradient descent method to adjust the parameter of membership function. The detail coverage of ANFIS can be found in (Jang, ; Jang, Sadjadian et al., . Due to its high interpretability and computational efficiency and built-in optimal and adaptive techniques, ANFIS is widely used in pattern recognition, robotics, nonlinear regression, nonlinear system identification and adaptive system processing and also it can be used to predict the inverse.

3. FORWARD KINEMATICS AND INVERSE KINEMATICS

In This section of the thesis the forward kinematics and the inverse kinematics of the 5-DOF and 7-DOF redundant manipulator is discussed. The Denavit-Hartenberg (D-H) notation for these two manipulators is discussed with steps used for deriving the forward kinematics is presented. Then this chapter is concluded with the solution of inverse kinematics for the 5-DOF redundant manipulator is given. The forward kinematics is concerned with the relationship between the individual joints of the robot manipulator and the position (x,y, and z) and orientation (\square) of the end-effector. Stated more formally, the forward kinematics is to determine the position and orientation of the end-effector, given the values for the joint variables (\square_i , a_i , d_i , \square_i) of the robot. The joint variables are the angles between the links in the case of revolute or rotational joints, and the link extension in the case of prismatic or sliding joints. The forward kinematics is to be contrasted with the inverse kinematics, which will be studied in the next section of this chapter, and which is concerned with determining values for the joint variables that achieve a desired position and orientation for the end-effector of the robot. The above mention theory is explained diagrammatically in figure 3.0

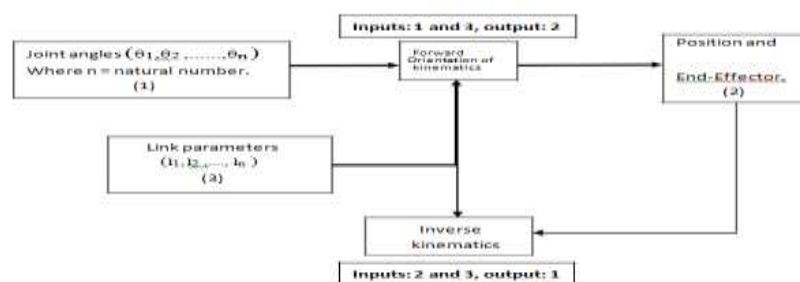


Figure 3.0 Forward and Inverse kinematics scheme

3.1 Denavit-Hartenberg Notation (D-H notation)

A Robot manipulator with n joints (from 1 to n) will have n + 1 links (from 0 to n, starting from base), since each joint connect to two links. By this convention, joint i connect link i - 1 to link i. It is considered that the location of the joint i to be fixed with respect to link i - 1. Each link of the robot manipulator is considered to be rigidly attached to a coordinate frame for performing the kinematics analysis. In particular, link i is attached to $o_i x_i y_i z_i$. It implies that whenever the robot executes motion, the coordinate of each point on the link I are constant when expressed in the $o_i x_i y_i z_i$ the coordinate frame. Furthermore when joint i actuate, link i and its attached frame $o_i x_i y_i z_i$, experience a resulting motion. The frame $o_0x_0y_0z_0$ is a inertial frame as it attached to the robot base. Now suppose, A_i is the homogeneous transformation matrix that express the position and orientation of $o_i x_i y_i z_i$ with respect to $o_{i-1}x_{i-1}y_{i-1}z_{i-1}$, where matrix A_i is not constant but varies as the configuration of the robot changes. Again the homogeneous transformation matrix that expresses the position and orientation of $o_j x_j y_j z_j$ with respect to $o_i x_i y_i z_i$ is called, by convention, a global transformation matrix and denoted by T_{ji} .

The following steps based on D-H notation are used for deriving the forward kinematics,

Step 1: Joint axes z_0, \dots, z_{n-1} are located and labelled

Step 2: Base frame is assigned. Set the origin anywhere on the z_0 axis. The x_0 and y_0 axes are chosen conveniently to form a right-hand frame.

Step 3: The origin O_i is located, Where the common normal to Z_i and Z_{i-1} intersects at Z_j . If Z_i intersects Z_{i-1} , a_i is located at the intersection. If Z_i, Z_{i-1} are parallel, located O_i in and convenient position along Z_i .

Step 4: x_i Considered along Common level between Z_{i-1} and Z_i the through O_i , or in the direction normal to the Z_{i-1} and Z_i intersect.

Step 5: y_i is established to complete a right-hand frame.

Step 6: The end-effector frame is assigned as on $x_n y_n z_n$. Assuming the n th joint is revolute, set $z_n = a_n$ along the direction z_{n-1} . The origin o_n is taken conveniently along z_n direction, preferably at the centre of the gripper or at the tip of any tool that the manipulator may be carrying.

Step 7: All the link parameters $\theta_i, a_i, d_i, \alpha_i$ are tabulated.

Where, $T_j^i = A_{i+1}A_{i+2} \dots A_{j-1}A_j$ if $i < j$

$T_j^i = I$ if $i = j$

$T_j^i = (T_i^j)^{-1}$ if $j > i$

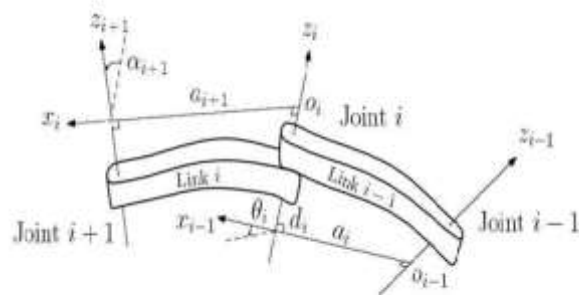


Figure 3.1. D-H parameters of a link i.e. $\theta_i, a_i, d_i, \alpha_i$

Step 8: The homogeneous transformation matrices A_i is determined by substituting the above parameters as shown in equation (1).

Step 9: Then the global transformation matrix ${}^0T_{End}$ is formed, as shown in equation (2).

This then gives the position and orientation of the tool frame expressed in base coordinates. In this convention, each homogeneous transformation matrix A_i is represented as a product of four basic transformations: $A_i = Rot(z, \theta_i)Trans(z, d_i)Trans(x, a_i)Rot(x, \alpha_i)$ Where four quantities $\theta_i, a_i, d_i, \alpha_i$ are parameter associate with link i and joint i. The four parameters $\theta_i, a_i, d_i, \alpha_i$ in the above equation are generally given name as joint angle, link length, link offset, and link twist.

3.2 The forward kinematics of a 5-DOF and 7-DOF Redundant manipulator.

3.2.1 Coordinate frame of a 5-DOF Redundant manipulator.

Table 1. Angle of rotation of joints

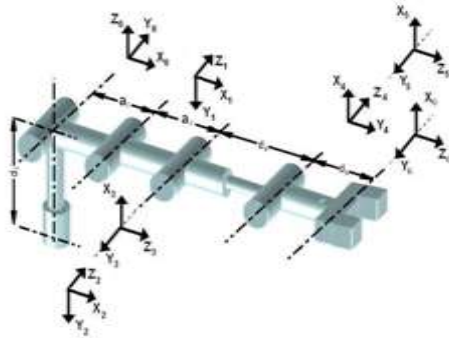


Figure 3.2.1B) Coordinate frame for the 5-DOF Redundant manipulator

Types of Joint	Range of Rotation
Rotating Base/ Shoulder (θ_1)	$0^\circ - 180^\circ$
Rotating Elbow (θ_2)	$0^\circ - 150^\circ$
Pivoting Elbow (θ_3)	$0^\circ - 150^\circ$
Rotating Elbow (θ_4)	$0^\circ - 85^\circ$
Pivoting Wrist (θ_5)	$15^\circ - 45^\circ$

3.2.2 Forward kinematics calculation of the 5-DOF Redundant manipulator.

Robot control actions are executed in the joint coordinates while robot motions are specified in the Cartesian coordinates. Conversion of the position and orientation of a robot manipulator end-effector from Cartesian space to joint space is called as inverse kinematics problem. The Denavit-Hartenberg (DH) notation and methodology is used to derive the kinematics of the 5-DOF Redundant manipulator. The coordinates frame assignment and the DH parameters are depicted in Figure 2 and listed in Table 2 respectively where (x_4, y_4, z_4) represents the local coordinate frames at the five joints respectively, (x_5, y_5, z_5) represents rotation coordinate frame at the end-effector where θ_i represents rotation about the Z-axis and transition on about the X- axis, d_i transition along the Z-axis, and a_i transition along the X-axis. The transformation matrix A_i between two neighbouring frames O_{i-1} and O_i is expressed in equation (1) as, $A_i = \text{Rot}(z, \theta_i) \text{Trans}(z, d_i) \text{Trans}(x, a_i) \text{Rot}(x, \alpha_i)$. By substituting the D-H parameters in Table 1 into equation (1), it can be obtained the individual transformation matrices A_1 to A_6 and the general transformation matrix from the first joint to the last joint of the 5-DOF Redundant manipulator can be derived by multiplying all the individual transformation matrices (0T_6). From equation (4) to (15), the position and orientation of the 5-DOF Redundant manipulator end-effector can be calculated if all the joint angles are given. This is the solution to the forward kinematics.

Table 2. The D-H parameters of the 5-DOF Redundant manipulator.

Frame	θ_i (degree)	d_i (mm)	a_i (mm)	α_i (degree)
$O_0 - O_1$	θ_1	$d_1 = 130$	$a_1 = 70$	-90
$O_1 - O_2$	θ_2	0	$a_2 = 160$	0
$O_2 - O_3$	$-90 + \theta_3$	0	0	-90
$O_3 - O_4$	θ_4	$d_4 = 140$	0	90
$O_4 - O_5$	θ_5	0	0	-90
$O_5 - O_6$	0	$d_6 = 120$	0	0

3.2.3 Work space for the 5-DOF Redundant manipulator.

Considering all the D-H parameters, the x, y and z coordinates are calculated for 5-DOF Redundant manipulator End-effector using forward kinematics equation shown in equations 4-15. For solving the forward kinematics equations, the angles of rotation of the joints are taken as tabulated in Table 1. Figure 4 shows the workspace for 5-DOF Redundant manipulator

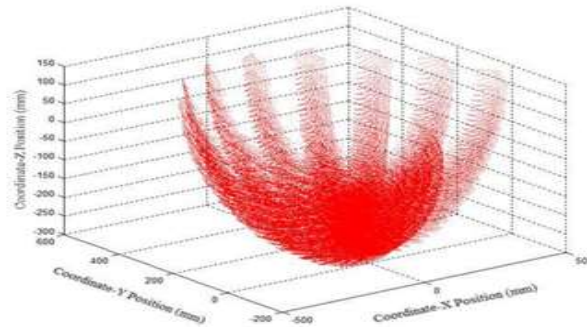


Figure 3.2.3 Work space for 5-DOF Redundant manipulator

3.2.4 Coordinate frame of a 7-DOF Redundant manipulator.

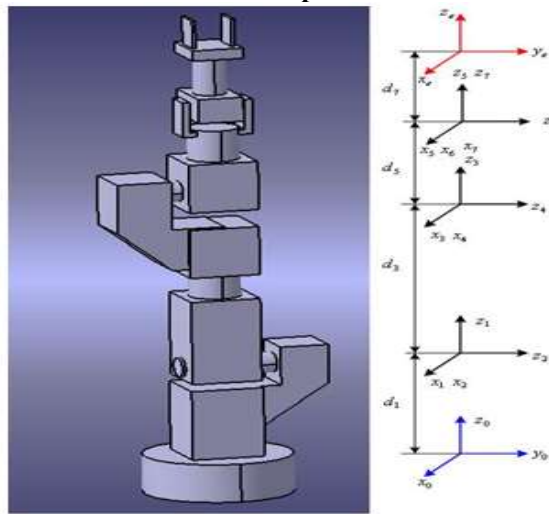


Figure:3.2.4 Coordinate frame for a 7-DOF Redundant manipulator

3.2.5 Forward kinematics calculation of the 7-DOF Redundant manipulator.

Table 3. The D-H parameters of the 7-DOF Redundant manipulator

frame	Link	θ_i (degree)	d_i (cm)	a_i (cm)	α_i (degree)
$o_0 - o_1$	1	$\theta_1 = -270$ to 270	$d_1 = 30$	0	0
$o_1 - o_2$	2	$\theta_2 = -110$ to 110	0	0	-90
$o_2 - o_3$	3	$\theta_3 = -180$ to 180	$d_3 = 35$	0	90
$o_3 - o_4$	4	$\theta_4 = -110$ to 110	0	0	-90
$o_4 - o_5$	5	$\theta_5 = -180$ to 180	$d_5 = 31$	0	90
$o_5 - o_6$	6	$\theta_6 = -90$ to 90	0	0	-90
$o_6 - o_7$	7	$\theta_7 = -270$ to 270	0	0	90
$o_7 - \text{End}$	End	-	$d_7 = 42$	0	0

3.2.6 Work space for the 7-DOF Redundant manipulator

Considering all the D-H parameters, the x, y and z coordinates (i.e. End effector coordinates) are calculated for 7-DOF Redundant manipulator using forward kinematics equation as shown in equations 17-28. For solving the forward kinematics equations, the angles of rotation of the joints are taken as tabulated in Table 2. Figure 6 shows the workspace for this manipulator.

3.3 Inverse kinematics of 5-DOF Redundant manipulator.

The forward kinematics equations (4)-(15) are highly nonlinear and discontinuous. It is obvious that the inverse kinematics solution is very difficult to derive. This paper uses various tricky strategies to solve the inverse kinematics of the 5-DOF robot manipulator. From equations (4) and (13), the following equation is derived: In solving the inverse kinematics solution of a higher DOF robot, a tan-1 function cannot show the effect of the individual sign for numerator and denominator but represent the angle in first or fourth quadrant. To overcome this problem and determine the joint in the correct quadrant, atan2 function is introduced in equations (31) and (32). Where the positive sign on the right hand side of the equation denotes for the elbow-out and the negative sign represents elbow-in configuration. The two solutions for the elbow-out and elbow-in of the 5-DOF Redundant manipulator are shown in the Figure 10. This process is being applied for θ_1 , θ_2 , θ_3 , θ_4 . To choose the correct solution, all the four sets of possible solutions (joint angles) calculated, which generate four possible corresponding positions and orientations using the forward kinematics. By comparing the errors between these four generated positions and orientations and the given position and orientation, one set of joint angles, which produces the minimum error, is chosen as the correct solution. The solutions (32), (50), (39), and (56) holds correct for obtaining the values of θ_1 , θ_2 , θ_3 , θ_4 respectively.

4. ANFIS ARCHITECTURE

ANFIS stands for adaptive neuro-fuzzy inference system developed by Roger Jang. It is a feed forward adaptive neural network which implies a fuzzy inference system through its structure and neurons. He reported that the ANFIS architecture can be employed to model nonlinear functions, identify nonlinear components on-line in a control system, and predict a chaotic time series. It is a hybrid neuro-fuzzy technique that brings learning capabilities of neural networks to fuzzy inference systems. It is a part of the fuzzy logic toolbox in MATLAB R2008a software of Math Work Inc. The fuzzy inference system (FIS) is a popular computing frame work based on the concepts of fuzzy set theory, fuzzy if-then rule, and fuzzy reasoning. It has found successful application in a wide variety of fields, such as automatic control, data classification, decision analysis, expert system, time series prediction, robotics, and pattern recognition. The basic structure of a FIS consists of 3 conceptual components: a rule base, which contains a selection of fuzzy rules; a database, which define the membership function used in fuzzy rules; a reasoning mechanism, which performs the inference procedure upon the rules and given facts to derive a reasonable output or conclusion. The basic FIS can take either fuzzy input or crisp inputs, but outputs it produces are almost always fuzzy sets. Sometime it is necessary to have a crisp output, especially in a situation where a FIS is used as a controller. Therefore, method of defuzzification is needed to extract a crisp value that best represent a fuzzy set. For solving the IK of 5-DOF and 7-DOF redundant manipulator used in this work Sugeno fuzzy inference system is used, to obtain the fuzzy model,. The Sugeno FIS was proposed by Takagi, Sugeno, and Kang in an effort to develop a systematic approach to generate fuzzy rules from a given input and output data set. The typical fuzzy rule in a Sugeno fuzzy model for three inputs used in this work for both the manipulator has the form:

The Grid partition method is often chosen in designing a fuzzy controller, which usually involves only several state variables as input to the controller. This partition strategy needs only a small number of membership functions for each input. However, it encounters problems when a large number of inputs are taken into consideration, leading to curse of dimensionality. Then the training of FIS is occurred, with some optimisation method like gradient descent and least square method. So, in this optimisation method, to explain the iteration and relationship between input and output of a system, a mathematical model is determined by observing its input and output data pairs, is generally refer to as system identification. The system identification includes the following steps.

- Specify and parameterize a class of mathematical model representing the system to be identified.
- Perform parameter identification to choose the parameters that best fit the training data.
- Conduct validation tests to see if the model identified responds correctly to an unseen data set.
- Terminate the procedure once the results of the validation tests are satisfactory. Otherwise, another class of model is selected and steps 2 through step 4 are repeated.

The above mentioned layers for a first order Sugeno model can be describe in detail as follow. Here the Gaussian membership function is used for 7-DOF Redundant manipulator.

Layer 1: (Input layer) In this layer, each node is equal to a fuzzy set and output of a node in the respective fuzzy set is equal to the input variable membership grade. The parameters of each node determine the membership function (Gaussian membership function for this present work) form in the fuzzy set of that node.

Layer 2: (Product layer) The output of each node represents the weighting factor of rule or product of all incoming signals. In which μ_{A_i} is the membership grade of x in A_i fuzzy set and μ_{B_i} is the membership grade of y in fuzzy set B_i and μ_{C_i} is the membership grade of z in fuzzy set C_i . Here AND (Π) operator is used to product the input membership values.

Layer 3: (Normalization layer) Every node (circle) in this layer is a fixed node labelled as N . This layer is also called normalised layer. It calculates the ration of weight factor of the rule with total weight factor. Here ϕ_i is refer to as the normalised firing strength.

Layer 4: The output of every node is calculated by multiplying the normalised one with the consequent parameters (p_i, q_i, r_i) of the linear function.

Layer 5: The single node here is a fixed node, labelled as \square , which compute the overall output as the summation of all incoming signal.

Thus, from the above theory an adaptive network is constructed, which is functionally equivalent to Sugeno fuzzy model. Note that the structure of this adaptive network is not unique as by combining layer 3 and layer 4, an equivalent network can obtain with only four layers.

4.1 ANFIS Architecture used for 5-DOF Redundant manipulator.

The coordinates and the angles obtained from forward kinematics solutions are used as training data to train ANFIS network with the triangular membership function with a hybrid learning algorithm. For solving the inverse kinematics equation of 5-DOF Redundant manipulator, in this work, considers the ANFIS structure with first order Sugeno model containing 343 rules. For the neuro-fuzzy model used in this work, 1024 data points analytically obtained using forward kinematics, of which 776 are used for training and the remaining 248 are used for testing (or validating).

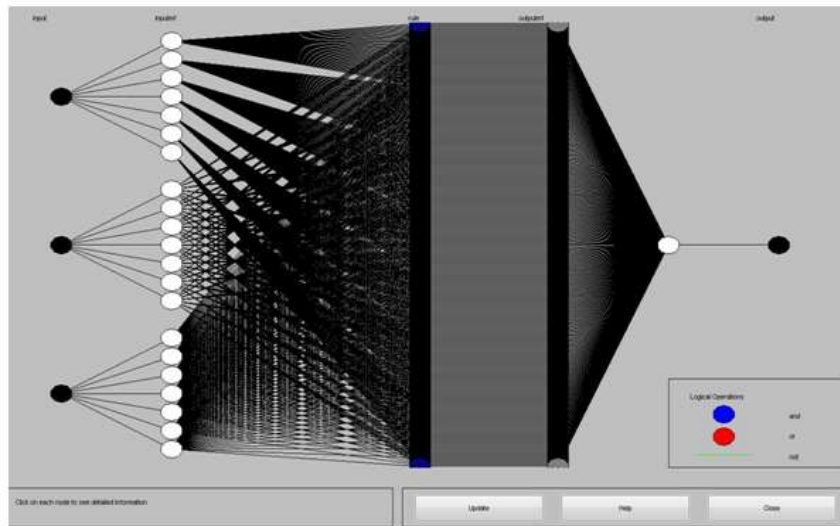


Figure:4.1 ANFIS model structure used for 5-DOF Redundant manipulator

The input is represented by the left-most node and the output by the right-most node. The node represents a normalization factor for the rules. Clicking on the nodes indicates information about the structure. To start the training, GENFIS1 function is used. GENFIS1 uses the grid partitioning and it generates rules by enumerating all possible combinations of membership functions of all inputs; this leads to an exponential explosion even when the number of inputs is moderately large. For instance, for a fuzzy inference system with 3 inputs, each with seven membership functions, the grid partitioning leads to 343 ($=7^3$) rules. GENFIS1 use a given training data set to generate an initial fuzzy inference system (represented by a FIS matrix) that can be fine-tuned via the ANFIS command. GENFIS1 produces a grid partitioning of the input space and a fuzzy inference system where each rule has zero coefficients in its output equation.

4.2 ANFIS Architecture used for 7-DOF Redundant manipulator.

For solving the inverse kinematics equation of 7-DOF Redundant manipulator, in this work, the grid partitioning option in the ANFIS toolbox is used. For each input, 7 membership function (Gaussian membership) are used along with 343 ($=7^3$) fuzzy rules are applied for all three inputs. For the neuro-fuzzy model used, 2187 data points are analytically obtained from MATLAB, of which 1640 are used for training and the remaining 547 are

used for testing (validating). The model structure for the 7-DOF Redundant manipulator used in ANFIS can be viewed as similar to the structure obtained for 5-DOF Redundant manipulator as discussed in the previous section. For obtaining the model for 7-DOF Redundant manipulator the Gaussian membership function with seven number of membership for each input is used as shown in following figure 14. The model structure obtained for 7-DOF manipulator. The Anfis information used for solving the 7-DOF Redundant manipulator for this work is tabulated in Table. 4.

Table 4. ANFIS information used for solving 7-DOF Redundant manipulator

3 inputs	: Cartesian coordinates: x, y, and z
1 output	: joint coordinate (θ)
7 member functions each input node	: Sugeno types
Number of nodes	: 734
Number of linear parameters	: 1372
Number of nonlinear parameters	: 42
Total number of parameters	: 1414
Number of training data pairs	: 1638
Number of checking data pairs	: 2187
Number of fuzzy rules	: 343

5. RESULT AND DISCUSSION

In this section of the thesis the surface plots, the residual plots and the normal probability plots for the 5-DOF and 7-DOF redundant manipulator is carried out. The surface plots obtained for this type of manipulators explains the efficiency of the ANFIS methodology. The residual plots obtained by comparing the predicted data from the ANFIS and the analytical data show that, the data predicted using ANFIS methodology deviate very less from the analytical data. The last section of this chapter is concluded with obtaining the normal probability plots. The details of the plots are explains in the following section.

5.1 3-D Surface viewer Analysis

In this section the 3-D surface plots, obtained for the 5-DOF and 7-DOF Redundant manipulator is discussed. The surface plot display both the connecting lines and faces of the surface in color. The surf command in MATLAB tool is use to create the 3-D surface plots of the matrix data. The surface plot explains the relation between the output and two inputs.

5.1.1 3-D Surface plots obtained for all joint angles of 5-DOF Redundant manipulator

Figures 15-19 show surface plot of five ANFIS networks relating inputs with joint angles of 5-DOF Redundant manipulator. Figure 15 indicates the surface plot between Cartesian coordinates y and z for θ_1 . It shows that when the values of y and z moving in a positive direction, there is a marginal increase followed by a decrease in θ_1 values. The inputs-output surface plot of θ_2 is shown in Figure 16. The Figure depicts that the value of θ_2 increases linearly when moving in the positive direction of y coordinate to some values of y and then there is a sudden increase of θ_2 values. No significant change in the value of θ_2 is observed with change in values of z coordinate. By moving from negative direction to the positive direction of x and y coordinates, the θ_3 value decreases first then followed by slightly increase, can be easily conclude from figure 17. Similarly the surface plot of θ_5 with input variables x and z coordinate is depicted in figure 19. It shows that the value of inputs has significant effect in determining the value of θ_5 . It concludes from the surface plot that the contribution of interdependent parameters toward obtaining the output can easily provide through the ANFIS algorithm and can be hardly obtained otherwise without employing, massive computations. All the surface viewer plots show that the total surface is covered by the rule base.

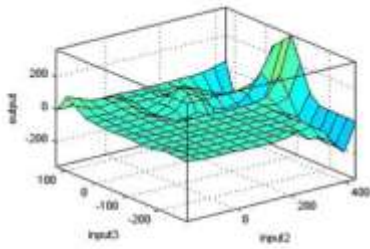


Figure : 5.1.1 A) Surface plot for θ_1

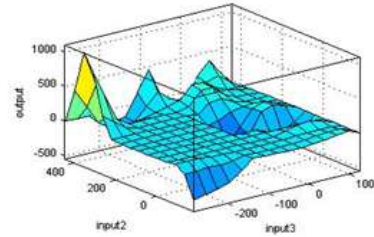


Figure : 5.1.1 D) Surface plot for θ_4

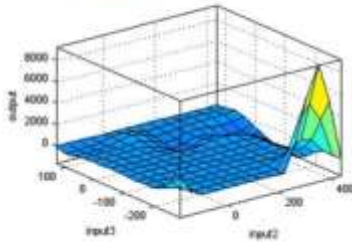


Figure : 5.1.1 B) Surface plot for θ_2

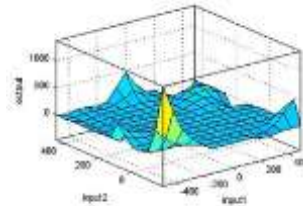


Figure : 5.1.1 C) Surface plot for θ_3

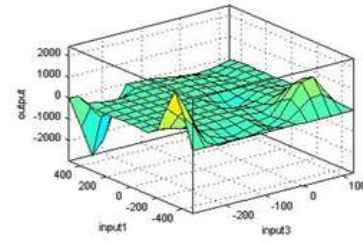


Figure : 5.1.1 E) Surface plot for θ_5

5.1.2 3-D Surface plots obtained for all joint angles of 7-DOF Redundant manipulator

The following Figure 19-25 shows the three dimensional surface plot of ANFIS network relating to the joint angle of 7-DOF Redundant manipulator. Figure 19 indicates the surface plot between Cartesian coordinates y and z for θ_1 . When the value of z decreases, there is a sudden increase in θ_1 value followed by decrease at the middle range of z value and there is no significant change in σ_1 value for y coordinate. The inputs-output surface plot of θ_2 is shown in Figure 20. The Figure depicts that the value of θ_2 decrease first followed by increase, for the increase in the value of z. No significant change in the value of θ_2 is observed with change in values of y coordinate. When y changes from positive value to negative value, there is a marginal increase in the value of θ_3 as well as there is no significant change with the value of z, as clearly noticed from Figure 21. With the increase in y value, at its middle range, the value of θ_5 decrease first then increase, where as there is no significant change for values of z, as depicted in Figure 5.1.2.A). Similarly, the 3 dimensional surface viewer for θ_4 , θ_6 , θ_7 can be explain. All the surface plots obtained from ANFIS, are continuous, smooth and the total surface is covered by the rule base.

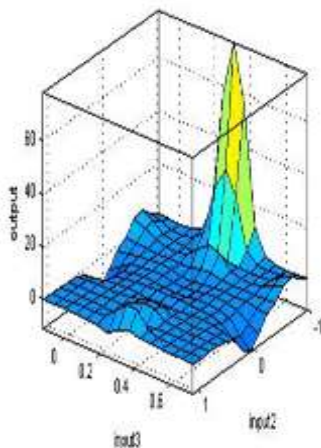


Figure :5.1.2 A), Surface plot for θ_1

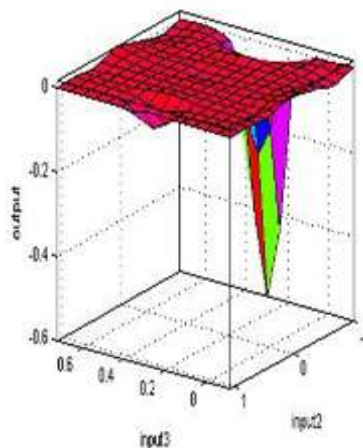


Figure :5.1.2 B), Surface plot for θ_2

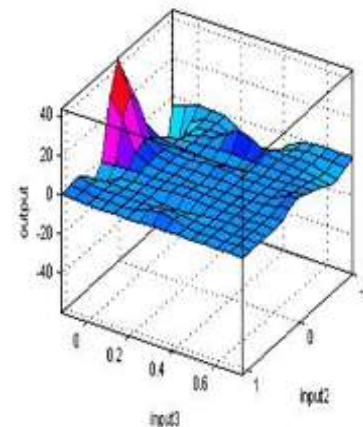


Figure :5.1.2 C) Surface plot for θ_3

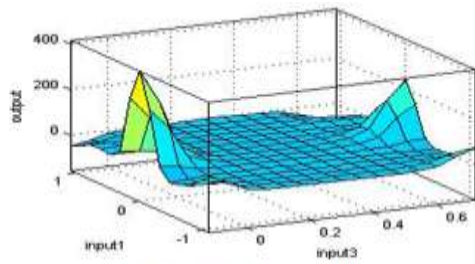


Figure :5.1.2 D) Surface plot for θ_4

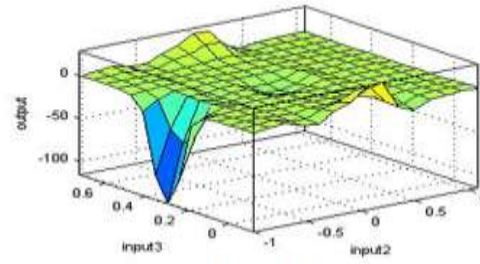


Figure 5.1.2 F) Surface plot for θ_6

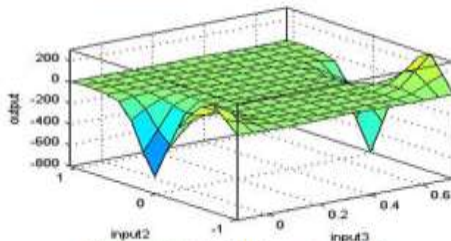


Figure :5.1.2 E) Surface plot for θ_5

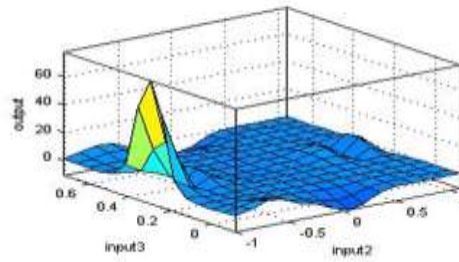


Figure 5.1.2 G) Surface plot for θ_7

5.2 Residual Plot Analysis

Residuals are the difference between the predicted output from the model (ANFIS) and the actual values of joint angles. The residual plot is a graph that shows the residuals in the vertical axis and the independent variables in the horizontal axis. If the points in the residual plot are randomly dispersed around the horizontal axis, the prediction model is considered to be appropriate for the data i.e. there is no drift in the data. In this section the residual plots are obtained for training and testing data of all joint angles of 5-DOF Redundant manipulator. It depicts the distribution of residuals of all joint angles are in the positive and negative axis of the plot. The residual plots for 5-DOF and 7-DOF are shown in following section.

5.2.1 The Residual plot of Training data for all joint angle of 5-DOF Redundant manipulator.

The residual plots of training data for θ_1 , θ_2 , θ_3 , θ_4 and θ_5 of 5-DOF Redundant robot manipulator are depicted in Figures 27-31 respectively. The residual plot shows a fairly random pattern as some of the residuals are in positive and some are lies in the negative side of the horizontal axis. Figure 27 shows a random pattern indicating a good fit for training data of θ_1 . As a very large number of residuals lie close to the horizontal axis shown in Figure 28, it indicates a reasonably good fit for θ_2 . The Figures 29-30 indicates a decent fit to the model of θ_3 and θ_4 as most of the residuals lie between -0.01 to 0.01. The Figure 31 explains the residual plot for training data of θ_5 . It indicates a few of the residuals of θ_5 lies beyond the range -0.1 to 0.1 and does not alter the prediction model of the data. The average absolute error (actual minus and predicted values) for the training data are found to be 0.0700, 0.0011, 0.0330, 0.0850, and 0.0240 for the joint coordinates θ_1 , θ_2 , θ_3 , θ_4 and θ_5 respectively. Similarly, the average absolute error of the testing data for the joint θ_1 , θ_2 , θ_3 , θ_4 and θ_5 are found to be 0.06, 0.03, 0.09, 0.10, and 0.11 respectively.

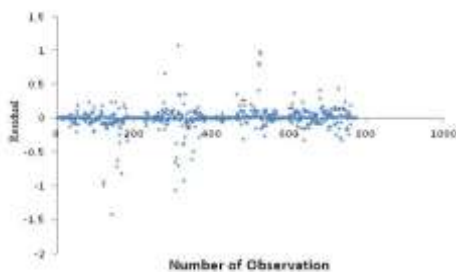


Figure 28. Residual plot of training data for θ_1

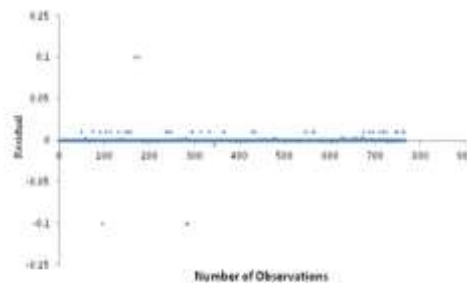


Figure 29. Residual plot of training data for θ_2

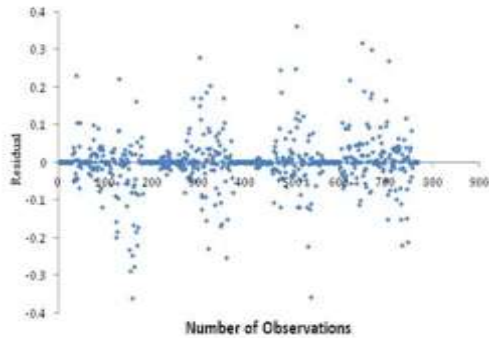


Figure 30. Residual plot of training data for θ_3

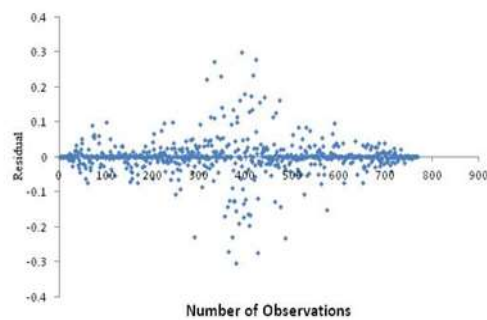


Figure 32. Residual plot of training data for θ_5

5.2.2 The Residual plot of Testing data for all joint angle of 5-DOF Redundant manipulator.

The residual plots of testing data for $\theta_1, \theta_2, \theta_3, \theta_4$ and θ_5 of 5-DOF Redundant robot manipulator are studied. The residual plot shows a fairly random pattern as some of the residuals are in positive axis and some are lies in the negative axis of the of the graph. Figure 32 shows a random pattern indicating a good fit for training data of θ_1 . As a very large number of residuals lie close to the horizontal axis shown in Figure 33, it indicates a reasonably good fit for θ_2 . The residuals for θ_3 lie between -0.2 to 0.2 and distributed over both sides of the mean line. It indicates that the prediction model is well suited for the study Figure 34. The Figures 35-36 indicates a decent fit to the model of θ_4 and θ_5 as most of the residuals lie between -0.03 to 0.03

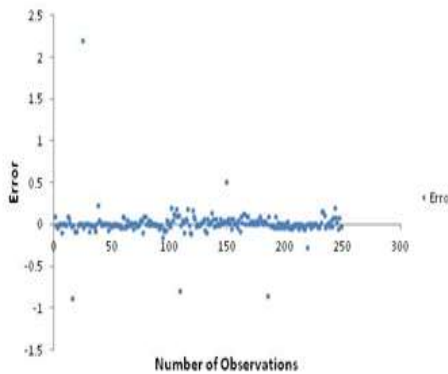


Figure 33. Residual plot of testing data for θ_1

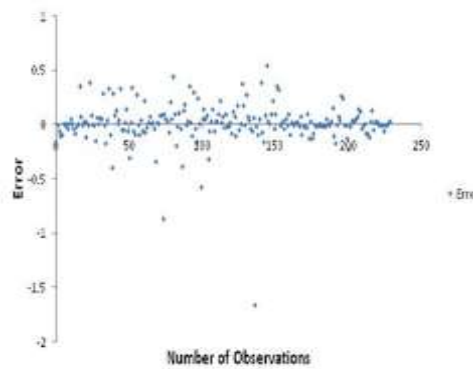


Figure 36. Residual plot of testing data for θ_4

5.2.3 The Residual plot of Training data for all joint angle of 7-DOF Redundant manipulator.

Similarly the residual plots of training data for $\theta_1, \theta_2, \theta_3, \theta_4, \theta_5, \theta_6,$ and θ_7 of 7-DOF redundant robot manipulator are studied. The residual plot shows a fairly random pattern as some of the residuals are in positive and some are lies in the negative side of the horizontal axis. Figure 37 shows a random pattern indicating a good fit for training data of θ_1 . As a very large number of residuals lie close to the horizontal axis shown in Figure 38, it indicates a reasonably good fit for θ_2 . The Figures 39-40 indicates a decent fit to the model of θ_3 and θ_4 as most of the residuals lie between -0.01 to 0.01. The Figure 41 explains the residual plot for training data of θ_5 . It indicates a few of the residuals of θ_5 lies beyond the range -0.1 to 0.1 and does not alter the prediction model of the data. The residual plots of training data for θ_6, θ_7 are depicted in Figure 42 and Figure 43.

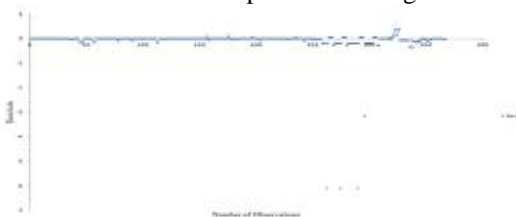


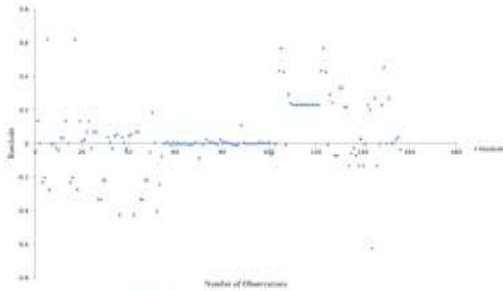
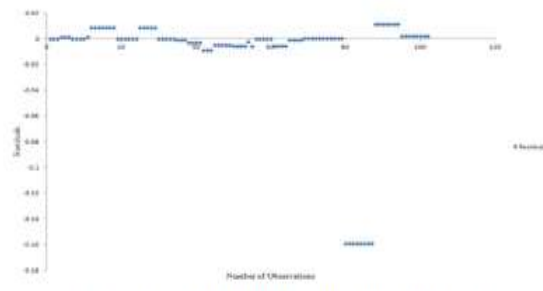
Figure 42. Residual plot of training data for θ_6



Figure 43. Residual plot of training data for θ_7

5.2.4 The Residual plot of Testing data for all joint angle of 7-DOF Redundant manipulator.

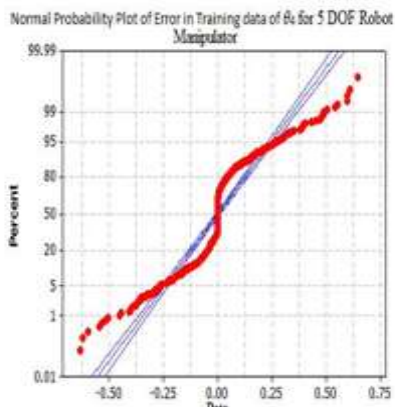
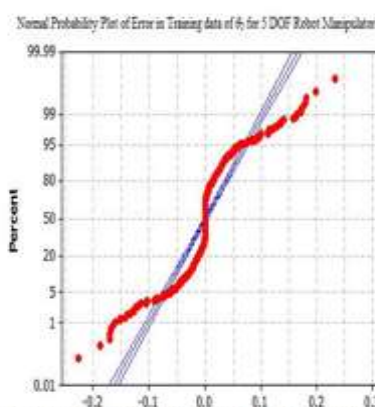
The residual plots of testing data for $\theta_1, \theta_2, \theta_3, \theta_4, \theta_5, \theta_6,$ and θ_7 of 7-DOF redundant robot manipulator are studied. The residual plot shows a fairly random pattern as some of the residuals are in positive axis and some are in the negative axis of the graph. Figure 32 shows a random pattern indicating a good fit for training data of θ_1 . As a very large number of residuals lie close to the horizontal axis shown in Figure 33, it indicates a reasonably good fit for θ_2 . The residuals for θ_3 lie between -0.2 to 0.2 and distributed over both sides of the mean line. It indicates that the prediction model is well suited for the study Figure 34. The Figures 35-36 indicate a decent fit to the model of θ_4 and θ_5 as most of the residuals lie between -0.03 to 0.03. The residual plot of θ_6 and θ_7 are presented in Figure 49 and Figure 50.

Figure 49. Residual plot of testing data for θ_5 Figure 50. Residual plot of testing data for θ_6

5.3 Normal Probability Plot Analysis

The normal probability plot is a graphical technique for assessing whether or not a data set is approximately normally distributed, if it is nearly straight, the data satisfy the nearly normal condition. The data are plotted against a theoretical normal distribution in such a way that the points should form an approximate straight line. Departures from this straight line indicate departures from normality. It provides a good assessment of the adequacy of the normal model for a set of data. It can also be defined as, in the normal probability plot, the normal distribution is represented by a straight line angled at 45 degrees. The actual distribution is plotted against this line so that any differences are shown as deviations from the straight line, making identification of differences quite apparent and interpretable. In this section, the normal probability plot of residuals of training and testing data of all joint angles for the 5-DOF and 7-DOF Redundant manipulator is depicted in the following Figures. The Anderson-Darling test (AD Test) is also carried out to compare the fit of an observed cumulative distribution function to an expected cumulative distribution function. Smaller the AD value, greater is the evidence that the data fit to the normal distribution. The following figures suggest that all the data are normally distributed. Similarly, the normal probability analysis is made for all training and testing data of all joint angles and signifies that the data are normally distributed.

5.3.1 Normal probability plot analysis of Training data for all joint angle of 5-DOF Redundant manipulator

Figure 55. Normal probability plot for residuals (Training data of θ_4)Figure 56. Normal probability plot for residuals (Training data of θ_5)

5.3.2 Normal probability plot analysis of Testing data for all joint angle of 5-DOF Redundant manipulator

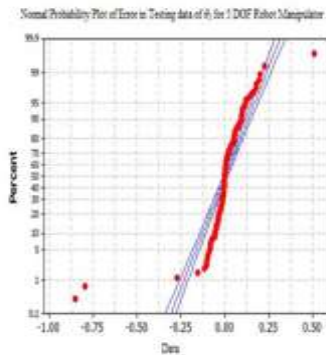


Figure 57. Normal probability plot for residuals (Testing data of θ_1)

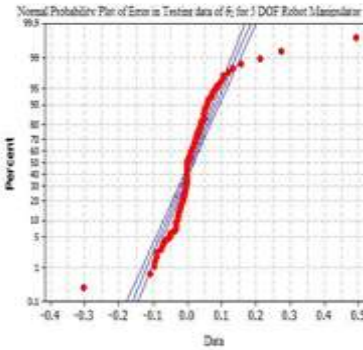


Figure 58. Normal probability plot for residuals (Testing data of θ_2)

5.3.3 Normal probability plot analysis of Training data for all joint angle of 7-DOF Redundant manipulator

The normal probability analysis of training and testing data for θ_3 , θ_5 , and θ_7 of 7-DOF Redundant manipulator is carried out in the following section similar to the 5-DOF Redundant manipulator. The data are plotted against a theoretical normal distribution in such a way that the points should form an approximate straight line. Departures from this straight line indicate departures from normality. It provides a good assessment of the adequacy of the normal model for a set of data. The Anderson-Darling test (AD Test) is also carried out similar to the 5-DOF Redundant manipulator, to compare the fit of an observed cumulative distribution function to an expected cumulative distribution function

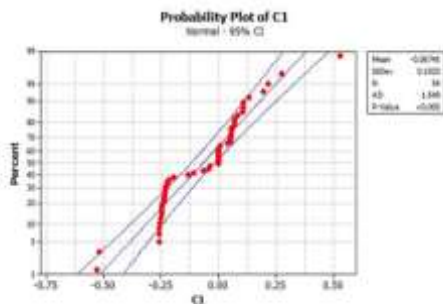


Figure 62. Normal probability plot for residuals (Training data of θ_3)

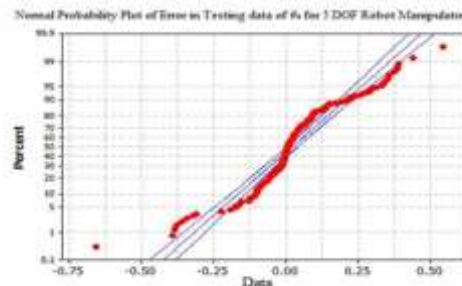


Figure 63. Normal probability plot for residuals (Training data of θ_5)

5.3.4 Normal probability plot analysis of Testing data for all joint angle of 7-DOF Redundant manipulator

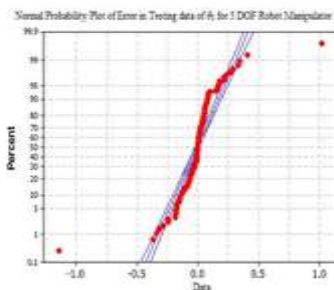


Figure 66. Normal probability plot for residuals (Testing data of θ_5)

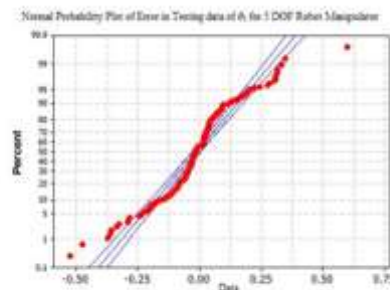


Figure 67. Normal probability plot for residuals (Testing data of θ_7)

5.4 Application of Artificial Neural Network (ANN)

In this work, an artificial neural network (ANN) model has also been adopted for estimating the IK solution of a 7-DOF redundant manipulator. A comparative study of both the techniques i.e ANFIS and ANN has been carried out. In this work, for the construction of model, 3-30-7 feed forward ANN, input layer consisting of 3

nodes, single hidden layer containing 20 nodes with tangent sigmoid activation function, and the output layer containing 7 nodes with linear activation function is used. The architecture of the neural network used in the analysis is shown in the Figure 68.

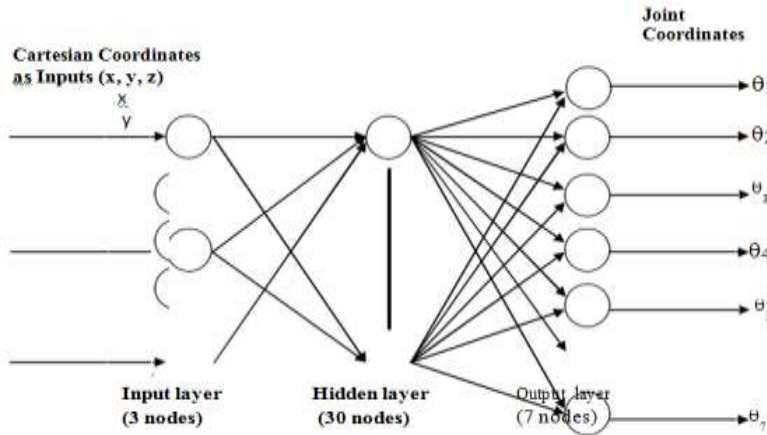


Figure 68. Schematic representation of Neural network used

In this analysis, MATLAB R2008a (Math Works, USA) software with its NN tool box is used for creating, training and testing the neural network. Here, 1638 data are taken as training and rest 549 data are taken as testing. The transfer function between input layer and hidden layer, hidden layer and output layer use tangent sigmoid function `tansig()` and linear function `purelin()` differently. Then, the learning rate (*lr*) is set to 0.07, MAX training steps epoch to 2000, show to 1000 and the Mean Square Error (MSE) of the network output as goal to 0.01.

Then the network is trained with `trainlm` function of L-M algorithm. In all the analyses, the ANFIS model result in the better prediction of the inverse kinematics solution of the 7-DOF redundant manipulators. The ANFIS model outperformed the ANN model and provides the best performance i.e., lowest MSE, lowest MBE and highest R2. The results of the study also indicate that the predictive capability of ANN models used is poor as compared to the ANFIS model used for solving inverse kinematics equation of 7-DOF redundant manipulator

Table 5. Performance of ANFIS model used

	θ_1		θ_2		θ_3		θ_4		θ_5		θ_6		θ_7	
	Tr	Ts	Tr	Ts	Tr	Ts	Tr	Ts	Tr	Ts	Tr	Ts	Tr	Ts
MSE	0.124	0.133	0.042	0.058	0.373	0.125	0.447	0.623	0.337	0.529	0.128	0.201	0.231	0.248
MBE	0.008	0.015	0.004	0.030	0.033	0.125	0.036	0.061	0.030	0.037	0.022	0.044	0.041	0.067
R ²	0.9918	0.9842	0.9826	0.9760	0.9958	0.9448	0.9907	0.9889	0.9956	0.9497	0.9925	0.9689	0.9998	0.9484

Table 6. Performance of ANN model used

	θ_1		θ_2		θ_3		θ_4		θ_5		θ_6		θ_7	
	Tr	Ts	Tr	Ts	Tr	Ts	Tr	Ts	Tr	Ts	Tr	Ts	Tr	Ts
MSE	1.06	0.524	0.142	0.492	1.59	1.14	2.15	2.25	0.366	0.93	1.62	1.48	1.91	1.82
MBE	0.025	0.030	0.009	0.030	0.069	0.083	0.079	0.116	0.031	0.150	0.077	0.088	0.118	0.183
R ²	0.9647	0.9666	0.9719	0.9370	0.9765	0.9675	0.9370	0.9178	0.9520	0.9150	0.9712	0.9248	0.9703	0.9323

ANFIS model are acceptable and very low (0.124, 0.042, 0.373, 0.128, 0.231 respectively) as compare to ANN model which are very high (1.06, 0.142, 1.59, 1.62, 1.91 respectively). So the ANFIS model is more flexible than the model of ANN considered in this study for the prediction of inverse kinematics solution. This can be justified as the ANFIS approach provides a general frame work for the combination of neural networks and fuzzy logic. So the ANFIS models perform better than the ANN models in the prediction of inverse kinematic solution for 7-DOF redundant manipulator.

By comparing the output from ANFIS and ANN model on the basis of global statistic i.e. MSE, MBE, and R2, it can be concludes that the ANFIS model is more flexible than the ANN model considered in this research, for prediction of IKs. As the ANFIS approach provides a general frame work for combination of NN and fuzzy logic. The efficiency of ANFIS over ANN can also be concluded by observing the graphs and tables which shows the comparison MSE, MBE, R2 for the two models. Based on comparison of the results of these two techniques, it is found that the proposed ANFIS model with Gaussian membership function is more efficient than the multilayer feed forward ANN using Levenberg-Marquardt (LM) algorithm for predicting the IK of the 7-DOF redundant manipulator.

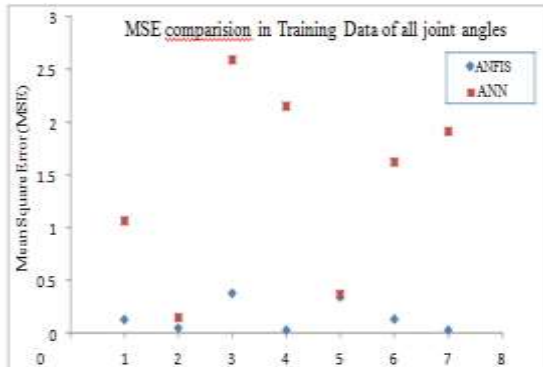


Figure 69. Comparison of Mean Square Error plot for Training data

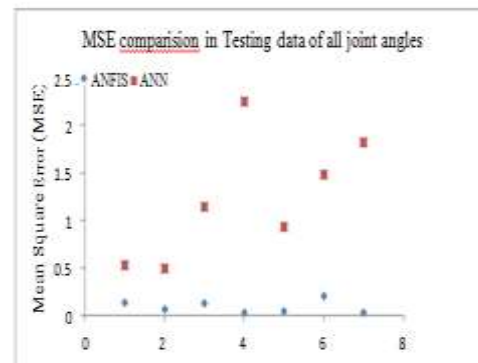


Figure 70. Comparison of Mean Square Error plot for Testing data.

6. CONCLUSION & FUTURE SCOPE

8.1 Conclusion

In this study, the inverse kinematics solution using ANFIS for a 5-DOF and 7-DOF Redundant manipulator is presented. The difference in joint angle deduced and predicted with ANFIS model for a 5-DOF and 7-DOF Redundant manipulator clearly depicts that the proposed method results with an acceptable error. The modelling efficiency of this technique was obtained by taking three end-effector coordinates as input parameters and five and seven joint positions for a 5-DOF and 7-DOF Redundant manipulator respectively as output parameters in training and testing data of NN models. Also, the ANFIS model used with a smaller number of iteration steps with the hybrid learning algorithm. Hence, the trained ANFIS model can be utilized to solve complex, nonlinear and discontinuous kinematics equation complex robot manipulator; thereby, making ANFIS an alternative approach to deal with inverse kinematics. The analytical inverse kinematics model derived always provide correct joint

As the ANFIS approach provides a general frame work for combination of NN and fuzzy logic. The efficiency of ANFIS for predicting the IK of Redundant manipulator can be concluded by observing the 3-D surface viewer, residual and normal probability graphs. The normal probability plots of the model are also plotted. The normal probability plot of residuals of training and testing data obtained from ANFIS shows that the data set of ANFIS are approximately normally distributed.

The methods used for deriving the inverse kinematics model for the these manipulators could be applied to other types of robotic arms, such as the EduBots developed by the Robotica Ltd, Pioneer 2 robotic arm (P2Arm), 5-DOF Lynx 6 Educational Robot arm. It can be concluded that the solution developed in this paper will make the Parm more useful in application with unpredicted trajectory movement in unknown environment.

8.2 Future Scope

In this work a hybrid neuro-fuzzy technology is used for the study of inverse kinematics of redundant robot manipulator. ANFIS is adopted for solving the IK of higher DOF robot manipulator. Due to its compactness and adaptive nature this technology is highly efficiency in predicting the IK of higher DOF robot manipulator. So this technology can used in different robot in different field to know the joint angles, orientations, and the robot working space to avoid osstacles.

The robotics industry has reached one plateau with the successful introduction of robots into automotive manufacturing for spot welding and painting, are two areas where robotic usage is almost universal. There are several other areas where the usage of robotics is in its infancy and this chapter is dedicated to brief descriptions of some of these fields along with a quick assessment of their current status.

A 20 meters long and 6-DOF remote robot manipulator is commonly used in space for repairing satellites and other coordinated activities on self-propelled platform. So ANFIS can be used to this robot for its free positioning and to determine its path. Apart from this, the neuro fuzzy technique can be used in various field to determine the positions and orientations. It can be used for: 1. Under water manipulator, 2. Nuclear, toxic waste disposal and mining robot 3. Firefighting, construction and agricultural robot, 4. Medical application

7. ACKNOWLEDGEMENTS

The Author would like to thank all the persons who helped in the completion of his experimental work. Also thanks are extended to ASR College of Engineering, Tanuku, West Godavari Dist, Andhra Pradesh, INDIA for support throughout the execution of the experimental work.

REFERENCES

- [1] Deb S.R. Robotics technology and flexible automation, Tata McGraw-Hill Publishing Company Limited. New-Delhi, 2008.
- [2] Clarke, R. Asimov's Laws of Robotics: Implications for Information Technology- part II, Computer, 27(1), September (1994): pp.57-66.
- [3] Martin, F.G. Robotic Explorations: A Hands-On Introduction to Engineering, Prentice Hall, New Jersey, 2001.
- [4] Featherstone R. Position and velocity transformations between robot end-effector coordinates and joint angles. International journal of Robotic Research, SAGE Publications, 2(2), (1983), pp. 35-45.
- [5] Nieminen and Peetu, et al. Water hydraulic manipulator for fail safe and fault tolerant remote handling operations at ITER, Fusion Engineering and Design, Elsevier, Vol. 84, (2009), pp. 1420-1424.
- [6] Hollerbach J.M. Optimum kinematic design for seven degree of freedom manipulator, Second International Symposium on Robotics Research. Cambridge: MIT Press, (1985): pp. 215-222.
- [7] Sciavicco L. and Siciliano B. Modelling and Control of Robot Manipulators, Springer Second edition, (2000), Chapter 3, pp. 96.
- [8] Shimizu M., Kakuya H. Yoon W, Kitagaki K., and Kosuge K., Analytical Inverse Kinematic Computation for 7-DOF Redundant Manipulators with Joint Limits and its application to Redundancy. Resolution, IEEE Transaction on Robotics, October (2008), 24(5).
- [9] Vassilopoulos A.P and Bedi R. Adaptive neuro-fuzzy inference system in modelling fatigue life of multidirectional composite laminates, Computation and Material Science.43 (2008): pp. 1086-1093. Haykin S., Neural Networks- A Comprehensive Foundation, McMillan College Publishing, New York, 1998.
- [10] Mendel J.M. Fuzzy logic system for engineering: A tutorial, Proceeding, IEEE. 83(3) (1995): pp. 345-377.
- [11] Ke L., Hong-ge M., Hai-jing Z. Application of Adaptive Neuro-Fuzzy Inference System to Forecast of Microwave Effect, IEEE Conference Publications, (2009), pp. 1- 3.
- [12] Alavandar S. and Nigam M. J. Adaptive Neuro-Fuzzy Inference System based control of six DOF robot manipulator, Journal of Engineering Science and Technology Review,1 (2008): pp.106- 111.
- [13] Craig J.J. Introduction to Robotics: Mechanisms and Controls, Addison-Wesley, Reading, MA, 1989.
- [14] Lee G.C.S. Dynamics and Control, Robot Arm Kinematics, Computer, 15(1982), Issue.12: pp. 62-79.
- [15] Korein J.U and Balder N.I. Techniques for generating the goal-directed motion of articulated structures', Institute of Electrical and Electronics Engineers Computer Graphics Applications, 2(1982), Issue. 9: pp.7181.
- [16] Srinivasan A and Nigam M.J. 'Neuro-Fuzzy based Approach for Inverse Kinematics Solution of Industrial Robot Manipulators', International Journal of Computers, Communications and Control, III(2008), No. 3: pp. 224-234.
- [17] Calderon C.A.A., Alfaro E.M.R.P, Gan J.Q. and Hu H. Trajectory generation and tracking of a 5-DOF Robotic Arm. CONTROL, University of Bath, (2004).
- [18] De X., Calderon C.A.A., Gan J.Q., H Hu. An Analysis of the Inverse Kinematics for a 5-DOF Manipulator, International Journal of Automation and Computing,(2) (2005): pp. 114-124.
- [19] Gan J.Q., Oyama E., Rosales E.M. and Hu, H. A complete analytical solution to the inverse kinematics of the Pioneer 2 robotic arm, Robotica, Cambridge University Press. 23(2005): pp. 123-129.
- [20] Hasan A.T. and Al-Assadi H.M.A.A. Performance Prediction Network for Serial Manipulators Inverse Kinematics solution Passing Through Singular Configurations, International Journal of Advanced Robotic Systems, 7(2010), No. 4: pp. 10-23.
- [21] Conkur E. S. and Buckingham R. Clarifying the definition of redundancy as used in robotics. Robotica, 15 No 5 (1997): pp. 583-586.
- [22] Chiaverini S. Singularity-robust task-priority redundancy resolution for real time kinematic control of robot manipulators. IEEE Transaction on Robotics Automation, 13 No 3 (1997): pp. 398-410.
- [23] Yoshikawa T. Foundation of Robotics: Analysis and Control. MIT Press (1988).
- [24] Braganza D., Dawson D.M., Walker I.D., and Nath N. Neural Network Grasping Controller for Continuum Robots. IEEE Conference on Decision Control, (2006): pp.6445-6449.



CITE AN ARTICLE

Rangarao, B. V., & Shekhar, B. C. (2018). SOLUTION OF INVERSE KINEMATICS IN A REDUNDANT MANIPULATOR BY USING ANFISPAPER TITLE. *INTERNATIONAL JOURNAL OF ENGINEERING SCIENCES & RESEARCH TECHNOLOGY*, 7(12), 294-313.

